Environ Sci Pollut Res (2017) 24:9859–9869
DOI 10.1007/s11356-016-7807-6

High added-value products from the hydrothermal carbonisation of olive stones

A.M. Borrero-López[1] · V. Fierro[1] · A. Jeder[1,2] · A. Ouederni[2] · E. Masson[3] · A. Celzard[1]

Received: 31 May 2016 / Accepted: 29 September 2016 / Published online: 21 November 2016

Abstract Olive stones (OS) were submitted to hydrothermal carbonisation (HTC) in order to evaluate the possibility of producing high added-value products, mainly furfural (FU) and 5-hydroxymethylfurfural (5-HMF) on one hand and hydrochars and carbons on the other hand. Temperature (160–240 °C), residence time (1–8 h), initial pH (1–5.5) and liquid/solid ratio (4–48 *w*/*w*) were systematically varied in order to study the main products and to optimise FU production. FU production yield up to 19.9 %, based on the hemicellulose content, was obtained. Other minor, but valuable, compounds such as 5-methylfurfural (5-MF) and some phenolic compounds were also produced. The hydrochar was carbonised at 900 °C, and the resultant carbon material was highly ultramicroporous with a peak of pore size distribution centred on 0.5 nm and a surface area as high as 1065 $m^2\ g^{-1}$, typical of most carbon molecular sieves.

Keywords Hydrothermal carbonisation · Olive stones · Furfural production · Hydrochar

Responsible editor: Philippe Garrigues

✉ V. Fierro
Vanessa.Fierro@univ-lorraine.fr

[1] Institut Jean Lamour, UMR CNRS-Université de Lorraine, no. 7198, ENSTIB, 27 rue Philippe Seguin, CS 60036, 88026 Epinal Cedex, France

[2] Ecole Nationale d'Ingénieurs de Gabès, Université de Gabès, Avenue Omar Ibn El Khattab, Zrig 6072, Tunisie

[3] Critt bois, 27 rue Philippe Seguin, BP 91067, 88051 Epinal Cedex 9, France

Introduction

Olive trees are extensively grown in Mediterranean countries such as Spain, Greece, Italy and Tunisia, and olive stones (OS) are among the multiple by-products that are obtained from olive oil production. Olive production in the Mediterranean basin is estimated to be around 19 million t according to the Food and Agriculture Organisation Corporate Statistical Database (FAOSTAT 2016). Nowadays, OS industrial uses are nearly exclusively limited to energy cogeneration, but other uses are also possible. In the present study, hydrothermal carbonisation (HTC) of OS, i.e. treatment in hot pressurised water, was suggested for producing high added-value products (Knežević 2009).

After submitting biomass to HTC, the resultant liquid fraction contains small molecules such as formic or acetic acids but also compounds with molecular weights higher than several thousand dalton. Out of them, furfural (FU) and 5-hydroxymethylfurfural (5-HMF) are among the most interesting ones. FU is industrially produced by acid hydrolysis of pentosans or directly from biomass (Dashtban et al. 2012), from 5-HMF (not obtained at high scale), from glucoses and from fructoses. Possible formation mechanisms are shown in Fig. 1a, where R is 'H' in the case of FU production from pentosan or 'CH_2OH' in the case of 5-HMF production from fructose (Zeistch 2000). Glucose can be converted into fructose in aqueous media over homogeneous and heterogeneous catalysts (Marianou et al. 2016) and through isomerisation in a wide temperature range (Kooyman et al. 1977), as shown in Fig. 1b.

FU can be used as fungicide or nematicide, in special adhesives or flavours, for refinery lubricant recovery or as precursor of 5-methylfurfural, furfuryl alcohol, tetrahydrofurfuryl alcohol and tetrahydrofuran (Raman and Gnansounou 2015). FU production is around 430,000 t per year (Raman and

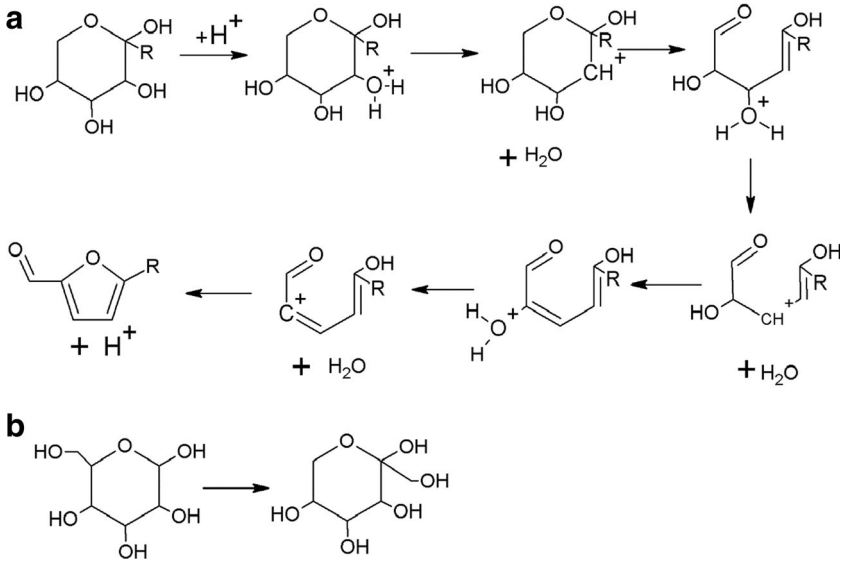

Fig. 1 **a** FU and 5-HMF reaction mechanism from pentosan (R = H) and fructose (R = CH_2OH), respectively. **b** Isomerisation of glucose to fructose

Gnansounou 2015), and its price is close to $1000 per ton (Yemis and Mazza 2012). The uses of 5-HMF are focused on substitutes of petroleum-based monomers for the production of fine chemicals and plastics, but industrial methods have not been developed yet (Chedda et al. 2007).

FU production from biomass has been extensively studied, and different processes have been carried out to achieve good yields. These processes are generally one-step and batch processes, although two-step processes (Raman and Gnansounou 2015; Riansa-Ngawong and Prasertsan 2011) and continuous processes (You et al. 2015) have been also proposed. FU yield was 3.3 wt% on dry basis after HTC of rice hull by using sulphuric acid as catalyst for 30 min at 125 °C and 1.5 atm, with a liquid/solid (L/S) ratio of 25 mL g^{-1} (Mansilla et al. 1998). Using a microwave-assisted process at 180 °C, L/S ratio of 100:1, pH 1.12 and 20 min of residence time, FU yields based on initial xylose were 48.4, 45.7 and 72.1 % for wheat straw, triticale straw and flax shives, respectively (Yemis and Mazza 2011). Faujasites and mordenites were used as catalysts for the production of FU (Moreau et al. 1998) and 5-HMF (Moreau et al. 1996). Xylose was submitted to HTC in water/toluene mixtures (*v*/*v* 1:3) at 170 °C, leading to a maximum yield of 34 and 42 % after 30 and 50 min of reaction, respectively (Moreau et al. 1998). 5-HMF was obtained from fructose when submitted to HTC by using water/methyl isobutyl ketone mixtures (*v*/*v* 1:5) at 165 °C. In this case, a maximum yield of 50 and 70 was achieved after 30 and 60 min, respectively (Moreau et al. 1996). Lactic acid was also used a catalyst for FU production from fructose (Agirrezabal-Telleria et al. 2011). Fructose was submitted to HTC in a 50 wt% lactic acid water solution at 150 °C for 2 h, and a 5-HMF yield up to 64 % was obtained (Lopes de Souza et al. 2012). FU production from OS in HTC conditions was also studied by Montané et al. (2002). These authors got up to 50–65 % of FU yield with respect to the initial pentosan content in the presence of sulphuric acid (0.05 to 0.250 mol L^{-1}) at a temperature between 220 and 240 °C and with 60–780 s of residence time.

The aforementioned studies only took liquid products into account. However, solid products from HTC processes are gaining increasing importance such as potential precursors of carbon-rich materials (Schneider et al. 2011; Braghiroli et al. 2012, 2014, 2015a,b,c). After hydrochar carbonisation, the carbon materials have applications in the fields of catalysis, electrochemistry, energy storage, selective gas sequestration, water purification or soil amendment (Steinbeiss et al. 2009; Titirici et al. 2012; Kang et al. 2012; Elmouwahidi et al. 2012; Li et al. 2014; Schaefer et al. 2016). In the present work, HTC of olive stones was carefully considered to obtain a better understanding of the effect of the process variables (i.e. temperature, time, initial pH and L/S ratio) on FU and 5-HMF production. The yield to hydrochar was also measured; one hydrochar also was pyrolysed, and the textural properties of the resultant carbon material were analysed.

Materials and methods

Raw materials

Olive stones (OS) were obtained from a local factory in Gabès, Tunisia. Lignin, cellulose and hemicellulose contents were determined according to the following Tappi standards: T 264, T 203 and T 222, respectively. OS were milled to a particle size smaller than 2 mm. Distilled water was used as reaction medium. Hydrochloric acid (0.1 mol L^{-1}, Sigma-Aldrich) was used to decrease the initial pH.

Hydrothermal carbonisation

HTC experiments were performed in 125-mL autoclaves (Anton Parr). The liquid (water) to solid weight ratio (L/S) was 8, i.e. 16 g of water and 2 g of OS, unless otherwise specified. Water and OS were both placed into a glass vessel, which was then introduced in the autoclave. The latter was next installed in a ventilated oven preheated at the desired temperature: 160, 170, 180, 190, 200, 220 or 240 °C, for different reaction times 1, 2, 4, 6 or 8 h. Once HTC was finished, the autoclaves were removed from the oven and left for cooling at room temperature for several hours.

Liquid and solid fractions were separated by vacuum filtration. The liquid fraction was weighed immediately after filtration and placed in a fridge until analysis. The solid fraction was first placed in a vacuum oven for 6 h at 60 °C for complete drying before being weighed accurately.

Taking as a reference the experimental conditions leading to the highest FU concentration, the pH was changed from 5.5 (natural pH) to 1 by adding 0.1 mol L^{-1} HCl solution. As the L/S ratio has a significant effect on the reaction products, it was set to 4/1, 6/1, 8/1, 12/1, 16/1, 24/1 and 48/1 (*w*/*w*). For all the experiments, 16 g of water was used.

Temperature and time are two critical components of liquid hot water (LHW) treatments. The reaction ordinate, $\log R_0$, based on the combination of temperature, T (°C), and residence time, t (min), was defined by Overend and Chornet (1987) to describe the impact of LHW treatments on lignocellulosic components:

$$\log R_0 = \log\left(t \cdot \exp\left(\frac{T-100}{14.75}\right)\right) \quad (1)$$

The activation energy based on the assumption that the reaction is hydrolytic and the overall conversion is first order is 14.75. The logarithm of the reaction ordinate, ($\log R_0$), is defined at the severity of the treatment or severity factor.

Liquid fraction analysis

The main compounds in the liquid fraction were identified by gas chromatography coupled with mass spectrometry (GC/MS) analysis by using a Clarus 500 GC/MS (PerkinElmer Inc.). Gas chromatography was carried out on a fused-silica capillary column (DB-5ms Ultra Inert; 30 m × 0.25 mm, 0.25-μm film thickness; Agilent J&W). The gas chromatograph was equipped with an electronically controlled split/splitless injection port. The injection (injection volume of 0.5 μL) was performed at 275 °C in the splitless mode with a 1-min splitless time. Helium (Alphagaz 2, Air Liquide) was used as carrier gas, with a constant flow of 1 mL min^{-1}. The oven temperature programme was as follows: 40 °C constant for 2 min, 40 to 325 °C at a rate of 7.5 °C min^{-1} and then 325 °C constant for 5 min. Ionisation was achieved under the electron impact mode (ionisation energy of 70 eV). The ion source and transfer line temperatures were 250 and 330 °C, respectively. Detection was carried out in scan mode: m/z 20 to m/z 500. The detector was switched off in the initial 5.5 min (solvent delay). Compounds were identified by comparison with spectra from the US National Institute of Standards and Technology (NIST) mass spectral library.

Furans and phenolic compounds were quantified by a Dionex Ultimate 3000 high-performance liquid chromatograph, equipped with auto sampler, diode array and fluorescence detectors trough (Thermo Scientific). A five-point calibration curve was carried out for each compound by using standard solutions, and values were accepted only when results get inside the values of the calibration curve, concentrating or diluting for that FU, 5-HMF and 5-methylfurfural (5-MF) were separated by using a Hypersyl Green PAH column (ThermoFisher Scientific). Four UV absorption wavelengths were used: 220, 276, 284 and 291 nm. Otherwise, fluorescence excitation and emission wavelengths were 360 and 443 nm, respectively. Mixtures of water and acetonitrile were used as mobile phases with water/acetonitrile volume ratios changing from 95:5 to 0:100 during the 35 min of the total duration of the experiment programme. In the first 1.5 min, a ratio of 95:5 was fixed. Then, from 1.5 to 15 min, the acetonitrile fraction increased linearly up to a ratio of 50:50 at 15 min. From 15 to 20 min, a linear increase was carried out until the ratio 0:100 was achieved, and this ratio was maintained for 5 min more. From 25 to 30 min, the acetonitrile amount decreased down to the initial ratio of 95:5 and was maintained 5 min until the end of the analysis.

Phenolic compounds were separated by using a Pinnacle DB Biphenyl (Restek) column. UV absorption wavelengths used were 195, 201, 231 and 300 nm. The mobile phases used were water and acetonitrile too. The programme started at 10 % of acetonitrile during the first 3 min. Later, the acetonitrile ratio increased up to 15 % at 5 min and remained the same until 13 min. From 13 to 15 min, the acetonitrile increased up to 20 % and remained constant for 13 min more. From 28 to 33 min, the ratio increased to 100 %. Until 38 min, 100 % of acetonitrile was kept. From 38 to 43 min, the acetonitrile decreased down to 10 % and remained constant until the end of the experiment at 50 min.

FU and 5-HMF yield assessment

Pentosans, such as xylose, and hexoses, such as glucose and fructose, are precursors of FU and 5-HMF, respectively, as already shown in Fig. 1a. As cellulose and lignin do not

produce FU, the FU yield is only related to hemicellulose content of OS and was therefore calculated from Eq. (2). 5-HMF, only related to cellulose content, was calculated from Eq. (3).

$$\text{FU Yield} = \frac{\text{FU massic concentration} \times \text{liquid volume}}{\text{mass of hemicellulose}} \quad (2)$$

$$\text{5-HMF Yield} = \frac{\text{5-HMF massic concentration} \times \text{liquid volume}}{\text{mass of cellulose}} \quad (3)$$

Hydrochar yield

Hydrochar yield was calculated as the ratio of hydrochar mass after vacuum drying to OS mass on dry basis (index 'db'), according to Eq. (4):

$$\text{Hydrochar Yield} = \left(\frac{\text{Hydrochar mass}}{\text{Initial Olive Stones mass}}\right)_{db} \quad (4)$$

Hydrochar carbonisation and carbon textural analysis

One hydrochar, prepared at 180 °C and 6 h, was carbonised under nitrogen flow (80 mL min^{-1}) in a tubular furnace. The heating rate was set at 1 °C min^{-1} up to 900 °C; dwell time was 3 h, and cooling was carried out under nitrogen flow.

Pore texture parameters were derived from nitrogen and carbon dioxide adsorption isotherms at −196 and 0 °C, respectively, by using a Micromeritics ASAP 2020 apparatus. Samples were degassed for 48 h under secondary vacuum at 270 °C. Surface area (S_{NLDFT}), micropore volume ($V_{\mu,NLDFT}$), as well as pore size distribution (PSD) were determined by application of the 2D non-local density functional theory (NLDFT) heterogeneous surface model (Jagiello and Olivier 2013) to both CO_2 and N_2 adsorption data by using the SAIEUS® routine provided by Micromeritics.

Results and discussion

Lignin, cellulose and hemicellulose contents in OS were found to be 29.88, 40.53 and 21.68 wt%, respectively.

Liquid fraction analysis

The optimisation of FU production was focused over a range of severity factors ($\log R_0$) ranging from 4.32 to 6.2 and centred on an average value of 4.91, which corresponds to standard time and temperature conditions of 6 h and 180 °C, respectively. All experimental conditions used in this work are presented in Table 1.

Figure 2 shows the GC/MS analysis of the liquid sample obtained after submitting OS to HTC at 190 °C for 4 h ($\log R_0$ = 5.03), where the maximum FU yield was obtained. Other compounds were, in order of appearance, 5-MF, 2,6-dimethoxyphenol, vanillin, 1-4-hydroxy-3-methoxyphenyl)-2-propanone (or 4-hydroxy-3-methoxyphenylacetone), 1-4-hydroxy-3-methoxyphenyl)-ethanone, 4-hydroxy-3,5-dimethoxy-benzaldehyde (or syringaldehyde) and 1-(2,4,6-trihydroxyphenyl)-2-pentanone. Especially interesting is 2,6-dimethoxyphenol, which is used as flavouring agent in food preparation and as substitute of phenol in phenol-formaldehyde resin, a commonly used adhesive for plywood (Bridgwater et al. 2008). Vanillin is used as flavour too, in perfumes, as a chemical intermediate in the production of pharmaceuticals and other fine chemicals and for developing thin layer chromatography plates (Esposito et al. 1997). Syringaldehyde is used in pharmaceuticals, food, cosmetics, textiles, pulp and paper industries and even in biological

Table 1 Experimental conditions used for optimising FU and 5-HMF production, as well as severity factors ($\log R_0$) and resultant FU and HMF concentrations and yields

Sample	$\log R_0$	[FU] (g L^{-1})	[FU] yield (%)	[5-HMF] (g L^{-1})	[5-HMF] yield (%)
160 °C, 6 h	4.32	2.62	6.64	0.08	0.15
170 °C, 2 h	4.14	0.05	0.12	0.002	0.005
170 °C, 4 h	4.44	2.65	6.72	0.07	0.13
170 °C, 6 h	4.62	5.99	15.20	0.20	0.37
180 °C, 2 h	4.43	0.26	0.67	0.01	0.018
180 °C, 4 h	4.74	5.73	14.53	0.19	0.36
180 °C, 6 h	4.91	7.50	19.02	0.34	0.64
190 °C, 4 h	5.03	7.61	19.30	0.32	0.59
190 °C, 6 h	5.21	6.55	16.62	0.62	1.17
190 °C, 8 h	5.33	6.18	15.69	0.50	0.94
200 °C, 2 h	5.02	4.64	11.77	0.08	0.14
200 °C, 4 h	5.32	7.01	17.78	0.55	1.04
200 °C, 6 h	5.50	4.39	11.14	1.06	1.98
220 °C, 2 h	5.61	4.10	10.39	0.78	1.47
240 °C, 1 h	5.90	1.90	4.83	0.27	0.50
240 °C, 2 h	6.20	2.44	6.18	1.78	3.35

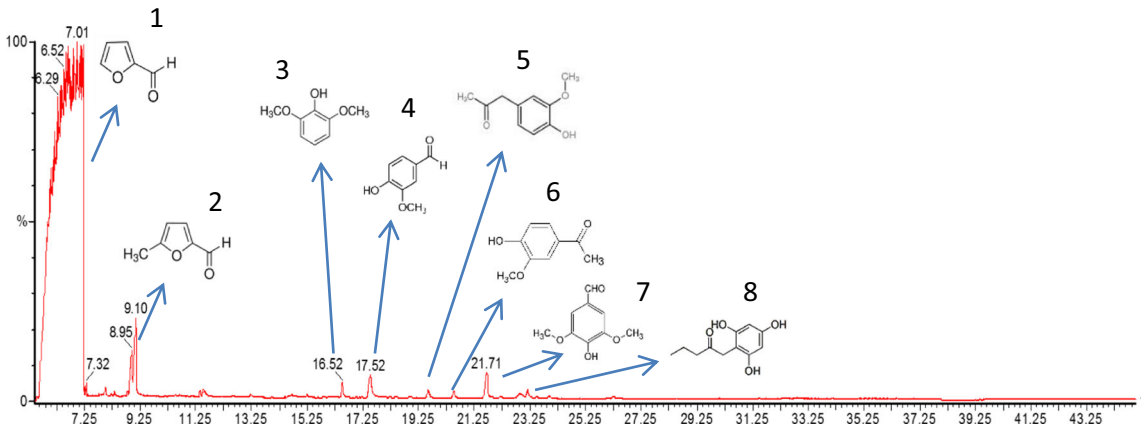

Fig. 2 Main products identified in the liquid fraction produced at logR_0 = 5.03 (190 °C; 4 h). FU (*1*), 5-HMF (*2*), 2,6-dimethoxyphenol (*3*), vanillin (*4*), 4-hydroxy-3-methoxyphenylacetone (*5*), 1-4-hydroxy-3-methoxyphenyl)-ethanone (*6*), syringaldehyde (*7*) and 1-(2,4,6-trihydroxyphenyl)-2-pentanone (*8*)

control applications (Nasir et al. 2012). Moreover, most of the aforementioned compounds are sold separately for fine chemical applications such as chromatography detection.

Effect of severity (logR_0)

Figure 3a, b shows the concentration of the two main products, FU and 5-HMF, as a function of logR_0. FU concentration increased until arriving to a maximum at 7.608 g L^{-1} at logR_0 = 5.03 (190 °C and 4 h) and decreased at higher logR_0. As for 5-HMF, no optimum was found but a strong increase of yield with logR_0. Thus, at the experimental conditions corresponding to the highest logR_0 = 6.20 (240 °C, 2 h), a maximum in the 5-HMF production was reached, 1.784 g L^{-1}. These results are in agreement with the literature. Hemicellulose degradation is indeed fast and starts at low temperatures: 60 min at 100 °C and 15 min at 180 °C produced a loss of 10 and 77.7 % of the initial hemicellulose content, respectively (Sun et al. 2014). Moreover, hemicellulose does not require high severity conditions to produce FU, which degrades when increasing values of logR_0 (Zeistch 2000). However, cellulose degradation is known to start above 200 °C (Gao et al. 2012), thereby explaining the low 5-HMF production. All results including

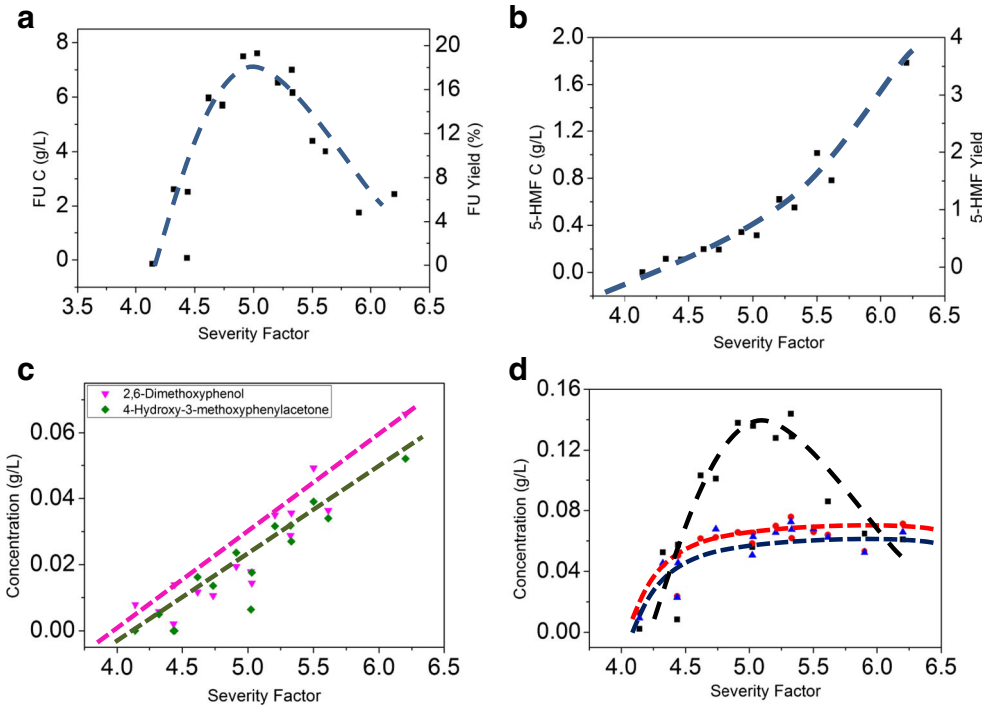

Fig. 3 Production of major compounds **a** FU and **b** 5-HMF and of minor compounds **c** 2,6-dimethoxyphenol and 4-hydroxy-3-methoxyphenylacetone and **d** 5-MF (*black*), vanillin (*red*) and syringaldehyde (*blue*) as a function of logR_0. For FU and 5-HMF, the yield is also indicated. *Dashed lines* are guides for the eyes

concentration and production yield of both compounds are shown in Table 1. The maxima in the FU and 5-HMF yields were 19.30 and 3.35 %, respectively, based on hemicellulose and cellulose contents in OS, respectively. Based on OS, the maxima were 4.18 and 0.98 %, respectively.

The maximum yield of 5-MF was found at $\log R_0 = 5.32$, i.e. close to that of FU, see Fig. 3d. This is due to the fact that FU and 5-MF are produced from hemicellulose and follow similar degradation paths. Vanillin and syringaldehyde showed an initial increase in their production with $\log R_0$, but a plateau was reached at $\log R_0$ higher than 4.9. In contrast, see Fig. 3c, 2,6-dimethoxyphenol and 4-hydroxy-3-methoxyphenylacetone concentrations increased linearly with $\log R_0$, and the maximum concentrations they could reach here were 0.0656 and 0.052 g L^{-1}, respectively, at the highest $\log R_0$ equal to 6.20. Phenolic compounds (vanillin, syringaldehyde, 2,6-dimethoxyphenol and 4-hydroxy-3-methoxyphenylacetone) are produced by lignin degradation, which occurs at more severe conditions than hemicellulose degradation.

Effect of pH

Acids have been widely used as catalysts in HTC processes, and it has been demonstrated that pH strongly affects FU and 5-HMF production (Yemis and Mazza 2012). Taking as a reference the experimental conditions leading to the highest FU concentration, 190 °C and 4 h, the pH was studied from 5.5 to 1. Figure 4a shows that higher fractions of FU and 5-HMF were obtained at lower pH, with optima at pH 2 and 1.5, respectively. Furfural yield reached 19.89 % at pH 2. Despite 5-HMF concentration increased by around three times from the initial natural pH, it was still lower than that obtained at 240 °C and 2 h. Once solid and liquid fractions were separated at the end of the experiment, the pH of the liquids was measured for observing whether pH changes might be related to FU and 5-HMF production. The corresponding data are shown in Fig. 4b: The highest FU concentrations were clearly obtained at the lowest final pH, whereas a maximum of 5-HMF was obtained at pH = 2.8, as shown in Fig. 4c.

As for minor compounds, i.e. 5-MF and phenolics, different behaviours were observed related to the initial pH, and they are shown in Fig. 4d. Just like for FU and 5-HMF, the production of 5-MF, vanillin and syringaldehyde was strongly affected by the initial pH. Thus, no 5-MF was detected when the initial pH was equal to 1. However, 2,6-dimethoxyphenol appeared to be not much affected by initial pH, whereas the production of 4-hydroxy-3-methoxyphenylacetone was the highest at low initial pH. Two opposite reactions may explain the different evolutions of product concentration. On one hand, hydronium ions facilitate dissolution and degradation of hemicellulose and lignin. On the other hand, high hydronium ion concentrations promote degradation. Therefore, 5-MF, vanillin and syringaldehyde concentrations sharply decreased when the initial pH decreased because degradation was more important. 4-Hydroxy-3-methoxyphenylacetone concentrations rose due to higher lignin degradation, while this product was affected by degradation in a lower extent when decreasing

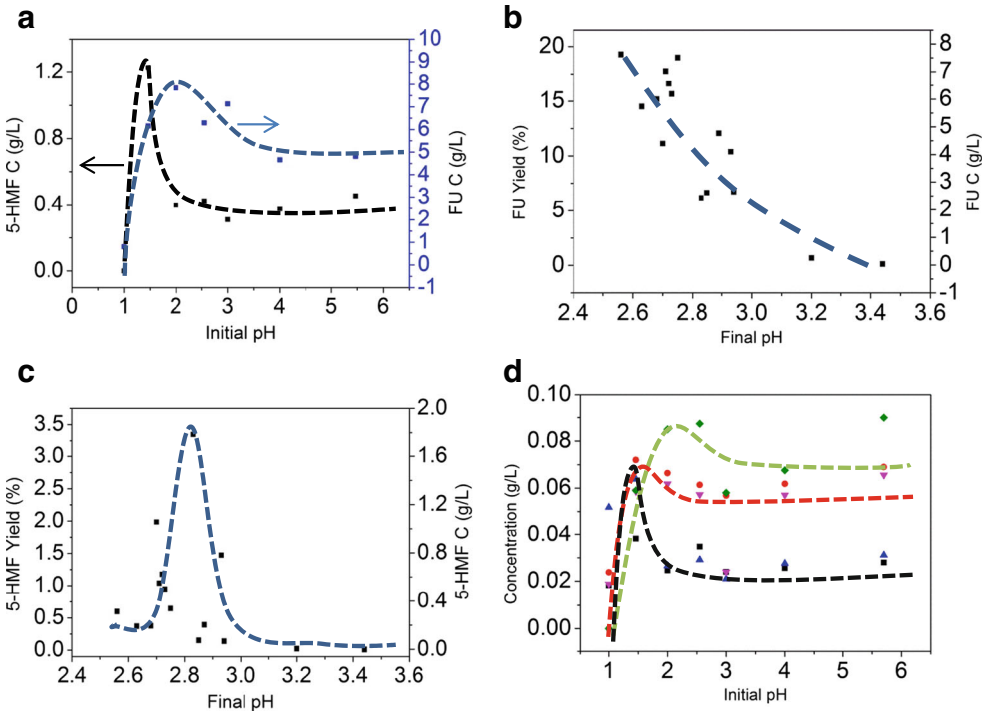

Fig. 4 **a** FU and 5-HMF concentrations as a function of initial pH. **b** FU concentration and yield as a function of final pH. **c** 5-HMF concentration and yield as a function of final pH. **d** 5-MF and phenolic compound concentrations (2,6-dimethoxyphenol (*black*), vanillin (*red*), 4-hydroxy-3-methoxyphenylacetone (*blue*), syringaldehyde (*pink*), 5-MF (*green*)), vs. initial pH. *Lines* are guides for the eyes

pH, and hence, 4-hydroxy-3-methoxyphenylacetone increased at lower pHs.

Effect of liquid/solid ratio

As seen in Fig. 5a–c, FU and 5-HMF concentrations and yields depend on the L/S ratio used, which plays a fundamental role in the reaction mechanisms. Figure 5a, c show FU and 5-HMF productions, respectively, as a function of the L/S ratio set to 4/1, 6/1, 8/1, 12/1, 16/1, 24/1 and 48/1 (*w*/*w*). FU and 5-HMF yields presented a steep maximum which was not expected from literature results. FU and 5-HMF highest yields were obtained at L/S ratios 24/1 and 12/1, respectively. This suggests that FU and 5-HMF production can be affected by interaction with other compounds and with themselves; therefore, too diluted solutions do not favour FU and 5-HMF production. However, too low L/S ratio decreases selectivity to FU, since it is known that FU can react with itself. The same behaviour is expected for 5-HMF. Hence, both FU and 5-HMF present production maxima as a function of L/S ratio.

Figure 5b shows FU concentrations as a function of L/S ratio for data reported in the open literature and compared with the maximum amount of FU obtained in the present work. The highest FU concentration obtained here, 7.608 g L^{-1}, was not far from that reported in other studies, although the L/S ratio was among the lowest ever used. Therefore, higher FU yields might certainly be obtained by increasing the L/S ratio. In this figure, the data presented at lower L/S ratios than ours were obtained with two-stage processes, which suggests that a pretreatment would be required to obtain an even higher FU production.

Figure 5d shows the production yield of 5-MF and of minor phenolic compounds. 5-MF, 2-methoxyphenol (2MP) and 2,6-dimethoxyphenol presented a maximum, i.e. the same trend as for FU and 5-HMF. The other three phenolic compounds exhibited an increase of yield when submitting more diluted samples to HTC. For vanillin and syringaldehyde, this increase was even higher than that of 4-hydroxy-3-methoxyphenylacetone. The observed behaviour for 5-MF, 2MP and 2,6-dimethoxyphenol can be explained in the same way as for FU and 5-HMF. On the other hand, the behaviour of vanillin, syringaldehyde and 4-hydroxy-3-methoxyphenylacetone can be explained by taking into account that these compounds are not favoured by interactions between the different molecules and themselves; therefore, an increase in concentration does not favour a rising yield; on the contrary, as water acts as catalyser, the higher is the water concentration, the higher is the production.

Solid fraction analysis

Figure 6a shows the hydrochar yield as a function of logR_0. By increasing logR_0, the hydrochar yield decreased and the hydrochar was correspondingly enriched in carbon due to the higher conversion of cellulose, hemicellulose and lignin at higher treatment time and temperature. The L/S ratio also had an important effect on the hydrochar yield obtained. Figure 6b shows that the hydrochar yield decreased

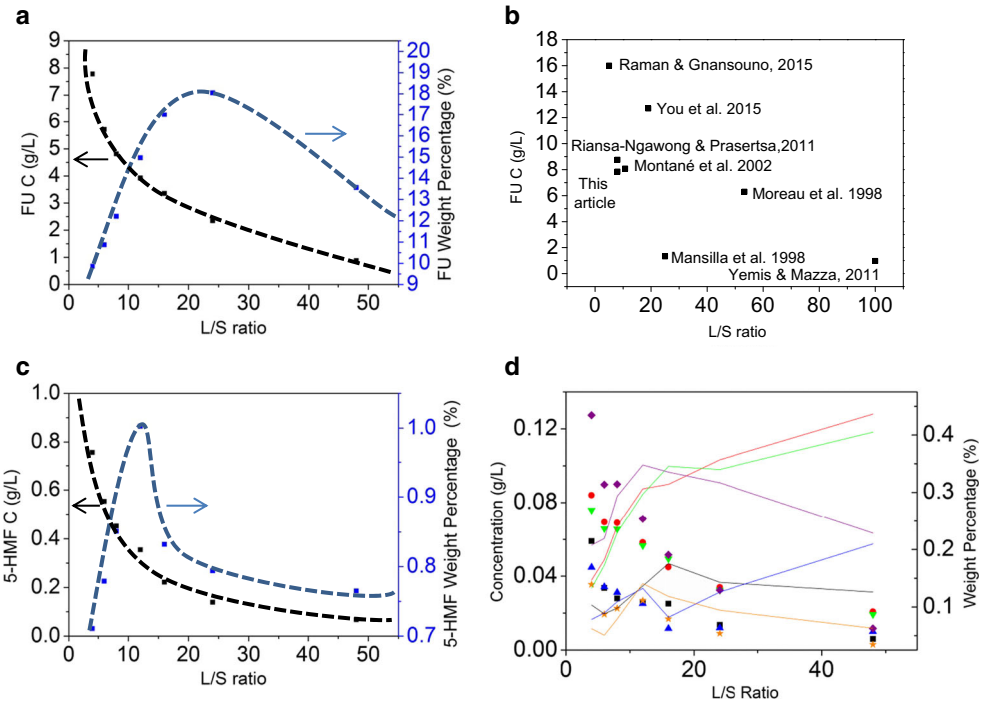

Fig. 5 Evolution with the L/S ratio of **a** FU concentrations and yield, **b** FU concentrations reported in literature compared to results obtained in this study (*dashed line*), **c** 5-HMF concentration and yield and **d** concentrations (*points*) and yields (*lines*) of minor compounds (2,6-dimethoxyphenol (*black*), vanillin (*red*), 4-hydroxy-3-methoxyphenylacetone (*blue*), syringaldehyde (*green*), 5-MF (*purple*) and 2-methoxyphenol (*golden*))

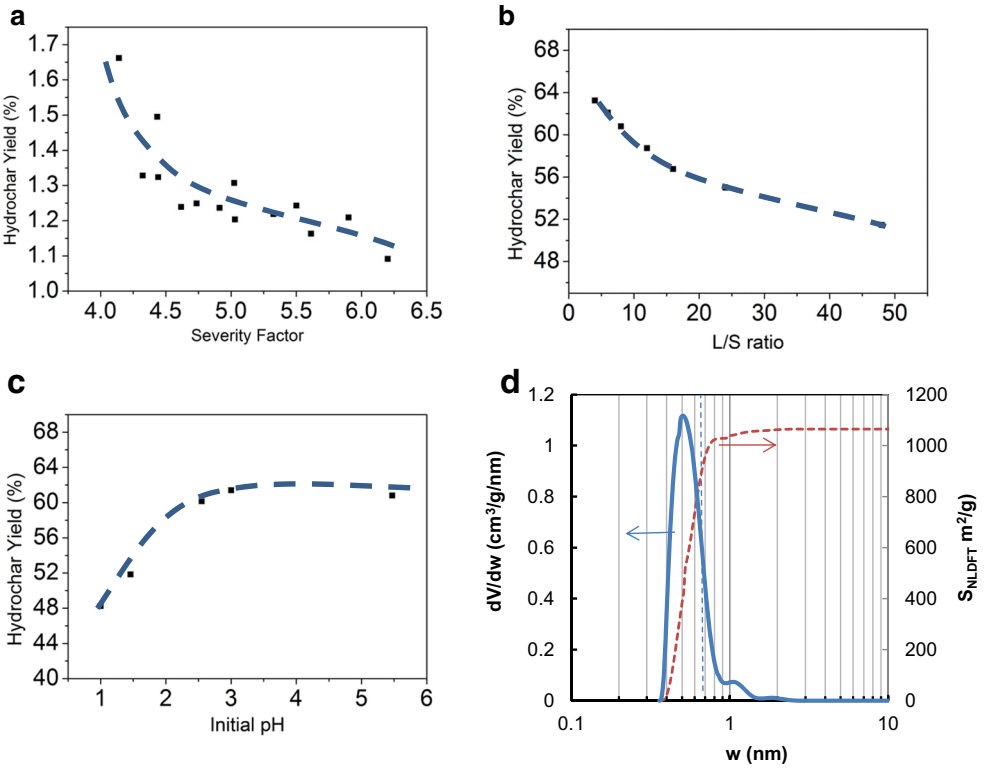

Fig. 6 Hydrochar yield as a function of **a** logR_0, **b** L/S ratio (the *solid line* is an exponential fit) and **c** initial pH. **d** Pore size distribution (PSD) and cumulated surface area of the carbon produced from hydrochar at logR_0 = 4.91. *Lines* are guides for the eyes in **a**, **b** and **c**

exponentially with the L/S ratio. Increasing the water fraction indeed favoured dissolution and kinetic reaction, due to the increase in the concentration gradient between water and OS; thus, a lower yield was obtained for higher L/S ratios (You et al. 2015).

Figure 6c shows that the hydrochar yield decreased when decreasing the pH below 3, due to hydrolysis and dehydration reactions (Lu et al. 2014). Finally, Fig. 6d shows the pore size distribution of the carbon produced after hydrothermal treatment at logR_0 = 4.91 and further pyrolysis under nitrogen

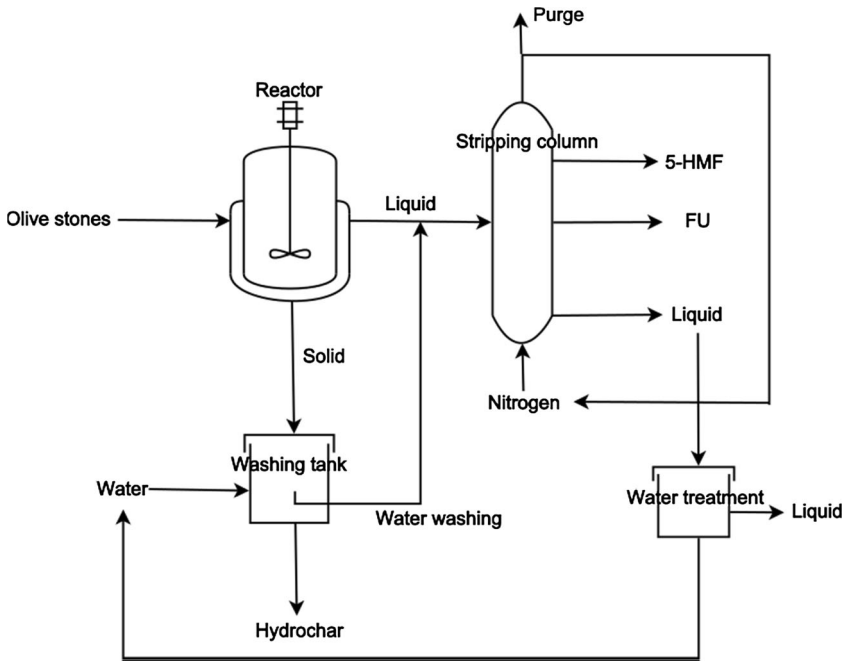

Fig. 7 Possible process diagram for simultaneous hydrochar, FU and 5-HMF production from olive stones

atmosphere at 900 °C. Nitrogen adsorption analysis was extremely slow, lasting up to 7 days due to the diffusional resistance at −196 °C, and the pore volume was not fully accessible to nitrogen. Textural surface properties were therefore assessed by nitrogen and carbon dioxide adsorption at −196 and 0 °C, respectively. The PSD of the resultant carbon materials was unimodal and narrow, centred on 0.5 nm, i.e. in the range of ultramicroporosity (pore diameter narrower than 0.7 nm). Total pore volume was equal to micropore volume; no mesoporosity (pore diameter between 2 and 50 nm) was detected. The surface area and the micropore volume (pore diameter narrower than 2 nm), calculated from the NLDFT model, were as high as 1065 $m^2\ g^{-1}$ and 0.26 $cm^3\ g^{-1}$, respectively. Most part of the microporosity was in the rage of ultramicropores and was equal to 0.22 $cm^3\ g^{-1}$. Therefore, the pyrolysis of OS-derived hydrochars produced ultramicroporous carbon materials with pore texture characteristics comparable to molecular sieves (CMSs) presently commercialised for gas separation. For instance, Carboxen 1003 (Sigma-Aldrich 2016) has a surface area of 1000 $m^2\ g^{-1}$, a micropore volume equal to 0.35 $cm^3\ g^{-1}$ and a pore diameter between 0.5 and 0.8 nm. The carbon materials produced here were not activated carbons (ACs), and they cannot be directly compared with them. ACs are produced by chemical or physical activation that develops the pore texture producing materials with higher surface area and wider PSD than those of CMSs. The carbon materials produced in this study, if they are not used as CMSs, could be further activated to obtain ACs similar to those previously reported in the abundant open literature (Ouederni et al. 2006; Spahis et al. 2008; Kula et al. 2008; Ghouma et al. 2015; Bohli et al. 2015).

Economic balance

There are about 850 million olive trees all over the world, whose space occupied is more than 10 million ha (ASEMESA 2016). Considering that around 15–25 wt% of the olive corresponds to the stone and taking only the Spain and Tunisia olive production, the production of OS would range from 1.5 to 2.5 million t. In Spain, the cost of OS is around 60–140 € t^{-1}, depending on variety and packaging (Olihueso 2016). The actual approximate prices for the main products that can be obtained from OS are \$50 g^{-1} for CMS (Sigma-Aldrich 2016), \$1200 t^{-1} for large-scale activated carbon production (Alibaba 2016), up to \$3000 t^{-1} for biochar fertiliser at small-scale production (Ecowarehouse 2016) and \$1000 t^{-1} for FU (Win 2005), which production is expected to double from 2013 to 2020 (Grand View Research 2016).

Keeping in mind that 60–65 % in weight could be obtained as hydrochar and 4 % as furfural, scaling up the present HTC process would therefore lead to 650 kg of a remarkable hydrochar and 40 kg of FU per ton of OS. Taking as a basis only the cost of fertiliser, FU and OS, great benefits could be obtained by HTC of OS. An accurate calculation of the investment and benefits should take into account operational and investment costs, as well as manpower, which are extremely variable from one country to another.

Figure 7 shows the scheme of a possible industrial process for producing both biochar and furfural. The reaction would take place in a batch reactor; the solid product would be washed, and the washing water with all the rest of the liquid would be treated for recovering FU and 5-HMF. The solid fraction might be used directly as fertiliser or for preparing activated carbons (Ubago-Pérez et al. 2006). FU and 5-HMF might be separated from HTC liquids in (i) a steam column, regarding their differences of boiling points, 162 and 116 °C for FU and 5-HMF, respectively, or (ii) in a stripping column by using nitrogen, which is considered as a cleaner alternative (Agirrezabal-Telleria et al. 2011). A further analysis of operational costs, waste treatment, as well as recovery of other interesting compounds and even valorisation of gas produced in HTC should be carried out in order to improve the energy and economic balance of the suggested process.

Conclusion

The treatment of OS in pressurised hot water, lately called HTC, allowed producing FU and 5-HMF as main products in the liquid phase, as well as a valuable solid product.

The highest FU yield was obtained at short times (4 and 6 h) and moderate temperatures (180 and 190 °C), while 5-HMF best yield was obtained in the hardest severity conditions (240 °C, 2 h) considered in this work. Moreover, pH and L/S ratio were shown to be important in obtaining higher yields; pHs 2 and 1.5 and L/S ratios of 24/1 and 12/1 were indeed found to be the best conditions for FU and 5-HMF production, respectively. The maximum FU production was close to 20 %, based on hemicellulose content in OS.

The solid phase consisted in a hydrochar likely to be exploitable for soil amendment or as precursors of highly porous carbon materials. Indeed, such hydrochar was shown to be easily converted into CMS by simple pyrolysis at 900 °C. Producing such kind of materials might even improve the economical balance of the process, as far as the cost of commercial CMS having very similar pore texture characteristics, i.e. extremely narrow pore size distribution and high surface area, is considered.

Acknowledgments A.M. Borrero-López acknowledges the training grant of the University of Granada (Spain) through ERASMUS+ programme. A. Jeder acknowledges the PhD and training grants of the University of Gabès (Tunisia) and the CHEERS (FEDER funds) project. Authors are grateful to CPER 2007–2013 'Structuration du Pôle de Compétitivité Fibres Grand'Est' (Competitiveness Fibre Cluster), through local (Conseil Général des Vosges), regional (Région Lorraine),

national (DRRT and FNADT) and European (FEDER) funds for the financial support.

References

Agirrezabal-Telleria I, Larreategui A, Requies J, Güemez MB, Arias PL (2011) Furfural production from xylose using sulfonic ion-exchange resins (amberlyst) and simultaneous stripping with nitrogen. Bioresource Technol 102:7478–7485. doi:10.1016/j.biortech.2011.05.015

Alibaba (2016) https://www.alibaba.com/showroom/activated-carbon-price.html accessed 28 May 2016

ASEMESA (2016) Asociación Española de Exportadores e Industriales de Aceitunas de Mesa http://www.asemesa.es/ accessed 28 May 2016

Bohli T, Ouederni A, Fiol N, Villaescusa I (2015) Evaluation of an activated carbon from olive stones used as an adsorbent for heavy metal removal from aqueous phases. Comptes Rendus Chimie 18(1):88–99. doi:10.1016/j.crci.2014.05.009

Braghiroli FL, Fierro V, Izquierdo MT, Parmentier J, Pizzi A, Delmotte L, Celzard A (2015c) High surface—highly N-doped carbons from hydrothermally treated tannin. Ind Crop Prod 66:282–290. doi:10.1016/j.indcrop.2014.11.022

Braghiroli FL, Fierro V, Parmentier J, Vidal L, Gadonneix P, Celzard A (2015b) Hydrothermal carbons produced from tannin by modification of the reaction medium: addition of H+ and Ag+. Ind Crop Prod 77:364–374. doi:10.1016/j.indcrop.2015.09.010

Braghiroli FL, Fierro V, Szczurek A, Stein N, Parmentier J, Celzard A (2015a) Electrochemical performances of hydrothermal tannin-based carbons doped with nitrogen. Ind Crop Prod 70:332–340 http://doi.org/10.1016/j.indcrop.2015.03.046

Braghiroli FL, Fierro V, Izquierdo MT, Parmentier J, Pizzi A, Celzard A (2012) Nitrogen-doped carbon materials produced from hydrothermally treated tannin. Carbon 50(15):5411–5420. doi:10.1016/j.carbon.2012.07.027

Braghiroli FL, Fierro V, Izquierdo MT, Parmentier J, Pizzi A, Celzard A (2014) Kinetics of the hydrothermal treatment of tannin for producing carbonaceous microspheres. Bioresour Technol 151:271–277. doi:10.1016/j.biortech.2013.10.045

Bridgwater AV, Effendi A, Gerhauser H (2008) Production of renewable phenolic resin by thermochemical conversion of biomass: a review. Renew Sust Energ Rev 12(8). doi:10.1016/j.rser.2007.04.008

Chedda JN, Roman-Leshkov Y, Dumesic JA (2007) Production of 5-hydroxymethylfurfural and furfural by dehydration of biomass-derived mono and poly-saccharides. Green Chem 9:342–350. doi:10.1039/B611568C

Dashtban M, Gilbert A, Fatehi P (2012) Production of furfural: overview and challenges. J Sci Technol Forest Prod Process 2:44–53

Ecowarehouse (2016) https://ecowarehouse.nz/ accessed 28 may 2016

Elmouwahidi A, Zapata-Benabithe Z, Carrasco-Marín F, Moreno-Castilla C (2012) Activated carbons from KOH-activation of argan (Argania spinosa) seed shells as supercapacitor electrodes. Bioresource Technol 111:185–190. doi:10.1016/j.biortech.2012.02.010

Esposito LJ, Formanek K, Kientz G, Mauger F, Maureaux V, Robert G, Truchet F (1997) Vanillin". Kirk-Othmer encyclopedia of chemical technology, 4th edition 24 edn. John Wiley & Sons, New York, pp. 812–825

FAOSTAT (2016) Food and Agriculture Organization of the United Nations Statistics division. http://faostat3.fao.org/home/E accessed 28 may 2016

Gao Y, Wang XH, Yang HP, Chen HP (2012) Characterization of products from hydrothermal treatments of cellulose. Energy 42:457–465. doi:10.1016/j.energy.2012.03.023

Ghouma I, Jeguirim M, Dorge S, Limousy L, Matei Ghimbeu C, Ouederni A (2015) Activated carbon prepared by physical activation of olive stones for the removal of NO2 at ambient temperature. Comptes Rendus Chimie 18(1):63–74. doi:10.1016/j.crci.2014.05.006

Grand View Research (2016) Furfural market analysis by application (furfuryl alcohol, solvent) and segment forecasts To 2020 http://www.grandviewresearch.com/industry-analysis/furfural-market accessed 28 may 2016

Jagiello J, Olivier JP (2013) Carbon slit pore model incorporating surface energetical heterogeneity and geometrical corrugation. Adsorption 19:777–783. doi:10.1007/s10450-013-9517-4

Kang S, Li X, Fan J, Chang J (2012) Solid fuel production by hydrothermal carbonization of black liquor. Bioresource Technol 110:715–718. doi:10.1016/j.biortech.2012.01.093

Knežević D (2009) Hydrothermal conversion of biomass. Dissertation, University of Twente

Kooyman C, Vellenga K, De Wilt HGJ (1977) The isomerization of d-glucose into d-fructose in aqueous alkaline solutions. Carbohydr Res 54(1):33–44. doi:10.1016/S0008-6215(77)80003-7

Kula I, Ugurlu M, Karaoglu H, Çelik A (2008) Adsorption of Cd(II) ions from aqueous solutions using activated carbon prepared from olive stone by ZnCl2 activation. Bioresour Technol 99(3):492–501. doi:10.1016/j.biortech.2007.01.015

Li L, Hale M, Olsen P, Berge ND (2014) Using liquid waste streams as the moisture source during the hydrothermal carbonization of municipal solid wastes. Waste Manag 34:2185–2195. doi:10.1016/j.wasman.2014.06.024

Lopes de Souza RL, Yu H, Rataboul F, Essayem N (2012) 5-Hydroxymethylfurfural (5-HMF) production from hexoses: limits of heterogeneous catalysis in hydrothermal conditions and potential of concentrated aqueous organic acids as reactive solvent system. Challenges 3:212–232. doi:10.3390/challe3020212

Lu X, Flora JRV, Berge ND (2014) Influence of process water quality on hydrothermal carbonization of cellulose. Bioresource Technol 154:229–239. doi:10.1016/j.biortech.2013.11.069

Mansilla HD, Baeza J, Urzfia S, Maturana G, Villasefior J, Durfin N (1998) Acid-catalysed hydrolysis of rice hull: evaluation of furfural production. Bioresource Technol 66:189–193. doi:10.1016/S0960-8524(98)00088-1

Marianou AA, Michailof CM, Pineda A, Iliopoulou EF, Triantafyllidis KS, Lappas AA (2016) Glucose to fructose isomerization in aqueous media over homogeneous and heterogeneous catalysts. Chem Cat Chem 8(6):1100–1110. doi:10.1002/cctc.201501203

Montané D, Salvadó J, Torras C, Farriol X (2002) High-temperature dilute-acid hydrolysis of olive stones for furfural production. Biomass Bioenergy 22:295–304. doi:10.1016/S0961-9534(02)00007-7

Moreau C, Durand R, Peyron D, Duhamet J, Rivalier P (1998) Selective preparation of furfural from xylose over microporous solid acid catalysts. Ind Crop Prod 7:95–99. doi:10.1016/S0926-6690(97)00037-X

Moreau C, Durand R, Razigade S, Duhamet J, Faugeras P, Rivalier P, Ros P, Avignon G (1996) Dehydration of fructose to 5-hydroxymethylfurfural over H-mordenites. Appl Catal A Gen 145:211–224. doi:10.1016/0926-860X(96)00136-6

Nasir M, Ibrahim M, Sriprasanthi RB, Shamsudeen S, Adam F, Bhawani SA (2012) A concise review of the natural existance, synthesis, properties, and applications of syringaldehyde. Bioresorcescom 7(3):4377–4399

Olihueso (2016) www.olihueso.es accessed 28 may 2016

Ouederni A, Souissi-Najar S, Ratel A (2006) Activated carbon from olive stones by a two step process. Influence of production parameters on textural characteristics 31(2):151–167. doi:10.3166/acsm.31.151-167

Overend RP, Chornet E (1987) Fractionation of lignocellulosics by steam: aqueous pretreatments. Phil Trans Royal Soc London A 32:523–536. doi:10.1098/rsta.1987.0029

Raman JK, Gnansounou E (2015) Furfural production from empty fruit bunch—a biorefinery approach. Ind Crop Prod 69:371–377. doi:10.1016/j.indcrop.2015.02.063

Riansa-Ngawong W, Prasertsan P (2011) Optimization of furfural production from hemicellulose extracted from delignified palm pressed fiber using a two-stage process. Carbohydr Res 346:103–110. doi:10.1016/j.carres.2010.10.009

Schaefer S, Fierro V, Izquierdo MT, Celzard A (2016) Assessment of hydrogen storage in activated carbons produced from hydrothermally treated organic materials. Int J Hydrog Energy 41(28):12146–12156. doi:10.1016/j.ijhydene.2016.05.086

Schneider D, Escala M, Kawin Supawittayayothin K, Tippayawong N (2011) Characterization of biochar from hydrothermal carbonization of bamboo. Int J Renew Energy Environ 2:647–652. doi:10.4028/www.scientific.net/AMM.654.7

Sigma-Aldrich (2016) http://www.sigmaaldrich.com/analytical-chromatography/ analytical-products.html?TablePage = 14540720

Spahis N, Addoun A, Mahmoudi H, Ghaffour N (2008) Purification of water by activated carbon prepared from olive stones. Desalination 222(1–3):519–527. doi:10.1016/j.desal.2007.02.065

Steinbeiss S, Gleixner G, Antonietti M (2009) Effect of biochar amendment on soil carbon balance and soil microbial activity. Soil Biol Biochem 41:1301–1310. doi:10.1016/j.soilbio.2011.04.022

Sun SN, Cao XF, Li HY, Xu F, Sun RC (2014) Structural characterization of residual hemicelluloses from hydrothermal pretreated Eucalyptus Fiber. Int J Biol Macromol 69:158–164. doi:10.1016/j.ijbiomac.2014.05.037

Titirici MM, White RJ, Falco C, Sevilla M (2012) Black perspectives for a green future: hydrothermal carbons for environment protection and energy storage. Energy Environ Sci 5:6796–6822. doi:10.1039/C2EE21166A

Ubago-Pérez R, Carrasco-Marín F, Fairén-Jiménez D, Moreno-Castilla C (2006) Granular and monolithic activated carbons from KOH-activation of olive stones. Microporous Mesoporous Mater 92:64–70. doi:10.1016/j.micromeso.2006.01.002

Win DT (2005) Furfural—gold from garbage assumption. Univ. J Technol 8(4):185–190

Yemis O, Mazza G (2011) Acid-catalyzed conversion of xylose, xylan and straw into furfural by microwave-assisted reaction. Bioresource Technol 102:7371–7378. doi:10.1016/j.biortech.2011.04.050

Yemis O, Mazza G (2012) Optimization of furfural and 5-hydroxymethylfurfural production from wheat straw by a microwave-assisted process. Bioresource Technol 109:215–223. doi:10.1016/j.biortech.2012.01.031

You SJ, Park N, Park ED, Park MJ (2015) Partial least squares modeling and analysis of furfural production from biomass-derived xylose over solid acid catalysts. J Ind Eng Chem 21:350–355. doi:10.1016/j.jiec.2014.02.044

Zeistch KJ (2000) The chemistry and technology of furfural and its many by-products. Elsevier Science BV, Amsterdam